Journal of Catalysis **189,** 339–348 (2000)
doi:10.1006/jcat.1999.2713, available online at http://www.idealibrary.com on IDEAL®

Redox and Chemisorptive Properties of Ex-Chloride and Ex-Nitrate $Rh/Ce_{0.6}Zr_{0.4}O_2$ Catalysts

2. Effect of High-Temperature Redox Cycling

Paolo Fornasiero, Neal Hickey, Jan Kašpar,[1] Tiziano Montini, and Mauro Graziani

Dipartimento di Scienze Chimiche, Università di Trieste, Via Giorgieri 1, 34127 Trieste, Italy

Received May 14, 1999; revised September 20, 1999; accepted September 20, 1999

The influences of high-temperature redox cycling and of the presence of chloride on the textural, redox, chemisorptive, and catalytic properties of $Rh/Ce_{0.6}Zr_{0.4}O_2$ were investigated by means of N_2 physisorption, volumetric hydrogen chemisorption, temperature-programmed reduction (TPR), temperature programmed desorption, and catalytic activity measurements of the reduction of NO by CO. This was achieved by conducting experiments on two samples of the material prepared from nitrate and chloride precursors. For the purposes of comparison, some parallel investigations were also conducted on the pure support. The results indicate that the precursor used does not affect the extent of vacancy creation upon application of identical high-temperature reduction procedures. However, the high-temperature reduction procedure used does have a detrimental effect on the position of vacancy creation during subsequent TPR profiles after mild reoxidation. Differences in behaviour due to the presence of chloride are detectable after application of such high-temperature reduction/mild reoxidation cycles, mainly in the chemisorption behaviour at low temperature and activity measurements under pseudo-steady-state conditions at 473 K. Significantly, severe ageing under reaction conditions does not eliminate differences in the rates of formation of products during the reduction of NO by CO.

Key Words: **rhodium nitrate; rhodium chloride; ceria–zirconia; chloride; redox properties; spillover; CO oxidation; NO reduction; three-way catalysts.**

1. INTRODUCTION

In Part 1 of this investigation the effect of low-temperature redox cycling on the interaction of H_2 with ex-nitrate and ex-chloride 0.5% $Rh/Ce_{0.6}Zr_{0.4}O_2$ catalysts was studied (1). The results showed that application of low-temperature cycling procedures affected the interaction of the ex-nitrate sample with H_2. The presence of chloride modified this behaviour and decreased the extent of low-temperature vacancy creation. Low-temperature redox cycling removed some chloride, which mainly affected the initial spillover behaviour. The present paper investigates the effect of high-temperature cycling on the same properties and extends the investigation to address the effect of the presence of chloride on the reduction of NO by CO.

2. EXPERIMENTAL

2.1. Catalyst Preparation and Standard Cleaning Procedure

The catalyst preparation and standard cleaning procedures have already been outlined in part 1 (1). The same three materials were investigated: $Ce_{0.6}Zr_{0.4}O_2$ and two 0.5 wt% $Rh/Ce_{0.6}Zr_{0.4}O_2$ samples prepared from nitrate and chloride precursors. These are designated CeZr, Rh/CeZr (N), and Rh/CeZr (Cl), respectively. Each sample was subjected to the cleaning procedure *in situ* before commencement of any experiment or series of experiments.

2.2. Analysis of Chloride Content

The chloride content of the samples was determined by a procedure already outlined (2). Aliquots of fresh and high-temperature cycled Rh/CeZr (Cl), aged according to the procedure outlined below, were analysed in this manner.

2.3. Hydrogen Chemisorption, Textural Analysis, and BET Surface Area Analysis

All chemisorption, textural analysis, and BET surface area measurements were conducted using a Micromeritics ASAP 2000 analyser. Typically 1 g of catalyst was used in such experiments.

H_2 chemisorption measurements were carried out at 308 and 195 K following the methodology already described (1). In certain cases oxidation treatments were administered to the samples before reduction. Details of the exact

[1] To whom correspondence should be addressed. E-mail: kaspar@univ.trieste.it. Fax: +39 040 6763903.

0021-9517/00 $35.00

pretreatment regimes applied to the samples before each measurement will be specified in the relevant text.

Textural analysis of the samples was conducted by measuring full adsorption isotherms at liquid N_2 temperature using N_2 as the adsorbate. These isotherms were recorded on fresh samples and after reduction at 1073 and 1273 K. These pretreatments are hereafter referred to as medium-temperature (MT) and high-temperature (HT) reduction.

2.4. Temperature-Programmed Experiments

Temperature-programmed reduction (TPR–MS) and temperature-programmed desorption (TPD–MS) experiments were conducted using the system already described (1). In the case of the TPR–MS measurements the same conditions as before were employed (0.2 g of catalyst, 5% H_2 in He, 10 K min^{-1}), the only difference being the final temperature reached (1273 K). Subsequent reoxidation was conducted in 5% O_2 in He from 700 to 423 K at a flow of 30 ml min^{-1}. Samples subjected to this redox cycle are hereafter referred to as high-temperature (HT) cycled. For all TPD–MS results presented in the present paper, H_2 adsorption (0.2 g of catalyst, 5% H_2 in He, 30 ml min^{-1}) was carried out at 308 K after ramping from room temperature (10 K min^{-1}). The samples were then cooled to room temperature in H_2/He and flushed with He (60 ml min^{-1}) before the TPD–MS procedure (60 ml min^{-1} He at 10 K min^{-1} to 873 K) was started. Details of the exact pretreatment regimes applied before each measurement will be specified in the relevant text.

TPR–TCD experiments were conducted under the same experimental conditions as the TPR–MS experiments using the apparatus referred to in part 1, using ca. 0.05 g of catalyst. As all of the TPR profiles were very similar, the TPR–TCD profiles are not included here. However, the results of quantification of the degree of reduction attained during the TPR are presented, as obtained by reoxidation at 700 K by pulsing O_2 until full recovery was observed.

2.5. Catalytic Activity Measurements

Reduction of NO (1% in He) by CO (3% in He) was used as a catalytic test of the Rh-loaded samples under investigation. Analysis was performed by online GC analysis using a Hewlett Packard 5890 Series II gas chromatograph equipped with a thermal conductivity detector. The use of two PLOT columns—Porapak Q and Hayesep A—and column switching allowed analysis of all possible products and reactants, i.e., CO_2, N_2O, N_2, O_2, CO, and NO. Activity measurements were conducted using ca. 0.05 g of catalyst supported on a quartz bed in a U-shaped quartz reactor, which was placed in a furnace. An additional layer of quartz was placed on top to act as a heat exchanger and therefore ensure thermal homogeneity of the reactive mixture passing over the catalyst bed. Measurements were first made isothermally at 473 K for 10 h before the furnace temperature was ramped from 473 to 1173 K at a rate of 1 K min^{-1}. Reaction temperature was monitored by means of a thermocouple located in the catalyst bed. A slightly rich CO–NO mixture (CO : NO = 1.2 : 1) was employed, with a total gas flow rate of 30 ml min^{-1} (GHSV = 12,500–50,000 h^{-1}). As the conditions were chosen so that measurements were in the kinetic regime, the first part of this procedure furnished pseudo-steady-state rates at 473 K, while the second part allowed determination of the light-off temperatures (the temperature of 50% conversion of the reactants).

Both $Rh/Ce_{0.6}Zr_{0.4}O_2$ samples were subjected to three consecutive activity measurement tests. After the first ramping procedure the temperature was held at 1173 K for 30 min before cooling to 473 K and initiation of the second test. At the end of this test the temperature was maintained at 1173 K for 10 h before cooling and the start of the third test. The aim of this repetition was to determine the effect of ageing under reaction conditions on the parameters measured.

3. RESULTS

3.1. Analysis of Chloride Content

The results of chemical analysis indicate a surface chloride content of 42 μmol g^{-1} on fresh Rh/CeZr (Cl) and of 16 μmol g^{-1} on a HT cycled sample.

3.2. Textural and BET Surface Area Analysis

A detailed investigation of the nature of the textural changes that occur upon reduction of CeZr, Rh/CeZr (N), and Rh/CeZr (Cl) at 1073 (MT) and 1273 K (HT) was conducted. These results are presented in Figs. 1 and 2 and in Table 1. It can be seen from Fig. 1 that Type IV isotherms with type H2 hysteresis loops were recorded for all of the fresh materials, indicating mesoporosity (3). Table 1 shows that the support has a higher surface area (50 m^2 g^{-1}) than the metal-loaded samples (38 m^2 g^{-1}). It should be noted that the Rh-loaded samples were subjected to an additional 5 h of calcination in air (773 K) after loading of the metal, which may have contributed to this decrease in surface area. In addition, as determined by *t*-plot analysis, the support has a higher incidence of micropores, as evidenced by the higher microporous area in Table 1. This difference is reflected in a marginally less pronounced hysteresis loop for the support in Fig. 1. As above, this may be partially attributed to the extra calcination step in preparation, but blocking of larger pores by Rh could also be a factor. However, the overall differences are rather small as the analysis also demonstrates that the mesopore volumes, the average pore diameters, and even the total micropore volumes are comparable for all three samples.

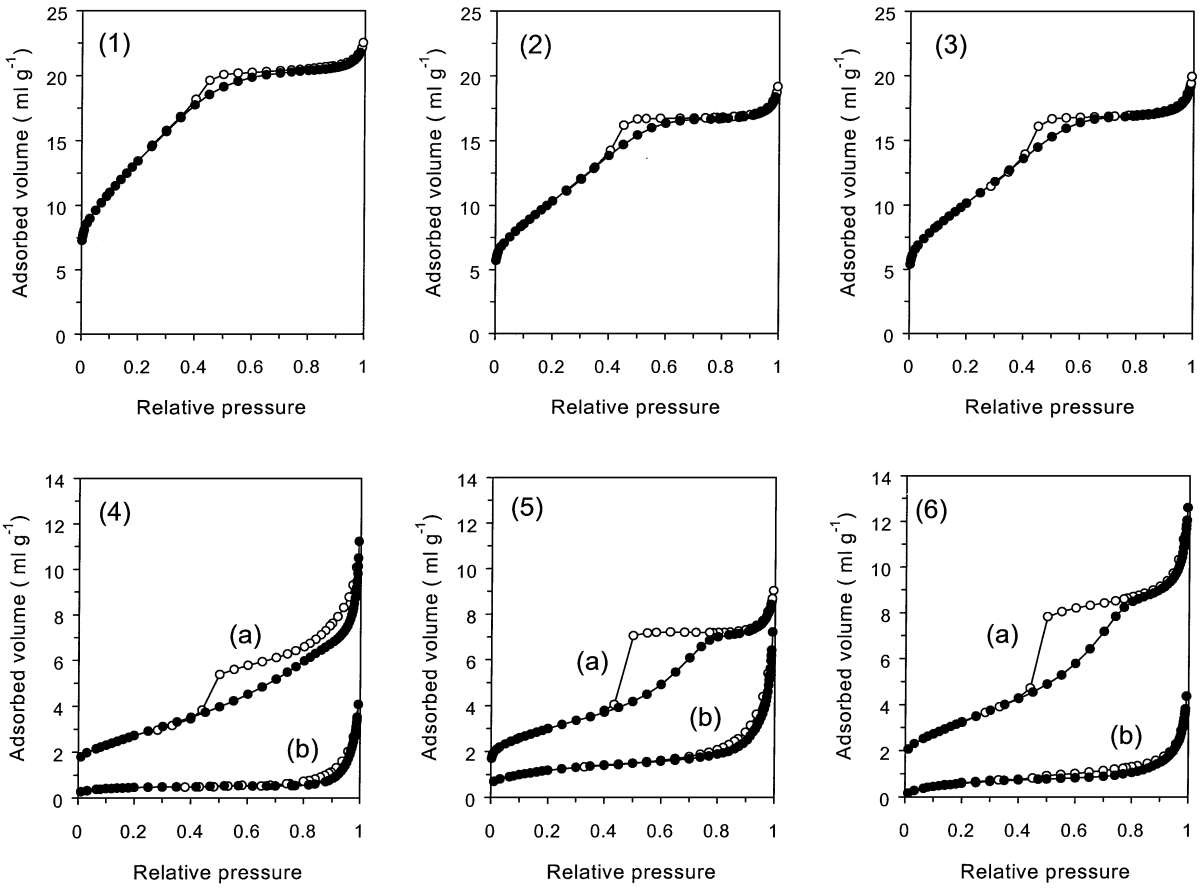

FIG. 1. N_2 adsorption isotherms at 77 K for $Ce_{0.6}Zr_{0.4}O_2$, $Rh/Ce_{0.6}Zr_{0.4}O_2$ (N), and $Rh/Ce_{0.6}Zr_{0.4}O_2$ (Cl): (1) $Ce_{0.6}Zr_{0.4}O_2$, fresh; (2) $Rh/Ce_{0.6}Zr_{0.4}O_2$ (N), fresh; (3) $Rh/Ce_{0.6}Zr_{0.4}O_2$ (Cl), fresh; (4) $Ce_{0.6}Zr_{0.4}O_2$, (a) after MT reduction and (b) after HT reduction; (5) $Rh/Ce_{0.6}Zr_{0.4}O_2$ (N), (a) after MT reduction and (b) after HT reduction; (6) $Rh/Ce_{0.6}Zr_{0.4}O_2$ (Cl), (a) after MT reduction and (b) after HT reduction.

MT reduction results in dramatic decreases of the surface areas of all samples. Table 1 indicates that the surface areas of CeZr, Rh/CeZr (N), and Rh/CeZr (Cl) decrease respectively to 10, 10, and 12 $m^2\ g^{-1}$. The shapes of the hysteresis loops also change significantly. Table 1 and Fig. 2, in which—following the BJH method (4)—the pore diameter of Rh/CeZr (N) is plotted against $dV/d\log(D)$ after each treatment, indicate that this is due to a change in the distribution of pores, with the average mesopore size increasing at the expense of micropores. These changes result in a decrease of the mesoporous volume of approximately 27–44%. Figure 2 is shown as an example of the behaviour observed upon MT and HT reduction. Very similar plots were obtained for all samples.

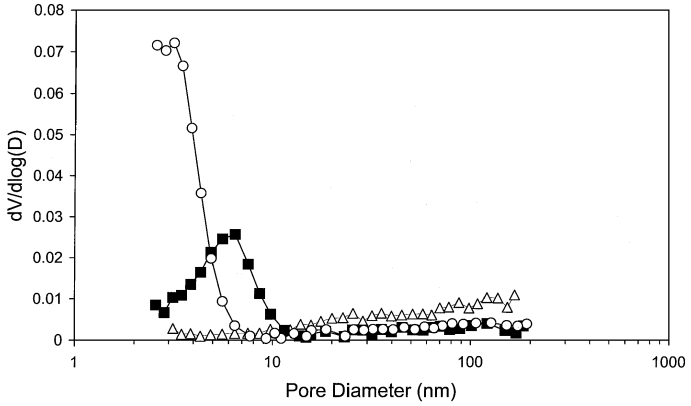

FIG. 2. Distribution of the mesopore diameter of $Rh/Ce_{0.6}Zr_{0.4}O_2$ (N) following the BJH method: (○) fresh, (■) after MT reduction and mild oxidation, and (△) after HT reduction and mild oxidation.

HT reduction further decreases the surface areas respectively for CeZr, Rh/CeZr (N), and Rh/CeZr (Cl) to 2, 4, and 2 $m^2\ g^{-1}$ (Table 1). Rh/CeZr (N) and Rh/CeZr (Cl) show some slight differences after MT and HT reduction; however, such differences are small and may be within the error of the technique. This treatment destroys completely the micro- and mesoporous structure of the samples (Figs. 1 and 2, Table 1). The hysteresis loops are poorly defined, and the shapes of the isotherms have changed from type H2 to type H3 typical of mesoporous materials lacking microporosity. These changes can also be seen from the changes of the average pore diameters and pore volumes (Table 1).

TABLE 1

Volumetric N_2 Adsorption on Fresh and Reduced (MT/HT) $Ce_{0.6}Zr_{0.4}O_2$ and $Rh/Ce_{0.6}Zr_{0.4}O_2$

Sample, reduction temperature[a,b] (K)	BET surface area ($m^2\ g^{-1}$)	Micropore area[c] ($m^2\ g^{-1}$)	$V_{micropores}$[c] ($ml\ g^{-1}$)	V_{BJH}[d] ($ml\ g^{-1}$)	Average pore diameter (Å)
$Ce_{0.6}Zr_{0.4}O_2$, fresh	50	43	0.03	0.027	34
$Ce_{0.6}Zr_{0.4}O_2$, 1073	10			0.017	
$Ce_{0.6}Zr_{0.4}O_2$, 1273	2			0.005	
$Rh(N)/Ce_{0.6}Zr_{0.4}O_2$, fresh	38	32	0.02	0.025	36
$Rh(N)/Ce_{0.6}Zr_{0.4}O_2$, 1073	10			0.014	
$Rh(N)/Ce_{0.6}Zr_{0.4}O_2$, 1273	4			0.008	
$Rh(Cl)/Ce_{0.6}Zr_{0.4}O_2$, fresh	38	31	0.02	0.026	38
$Rh(Cl)/Ce_{0.6}Zr_{0.4}O_2$, 1073	12			0.019	
$Rh(Cl)/Ce_{0.6}Zr_{0.4}O_2$, 1273	2			0.006	

[a] Pretreatment administered to the sample indicated after sample name. For the fresh sample this corresponds to oxidation (5% O_2 in He) at 900 K. In the other two cases this pretreatment was also applied before the samples were subjected to cycles of high-temperature reduction followed by mild reoxidation with O_2 pulses at 700 K. The samples used were prepared in this way before N_2 adsorption experiments.

[b] All the samples were degassed at 623 K prior to N_2 adsorption.

[c] Values determined from *t*-plots in the range $2 \times 10^{-5} - 0.1\ p/p_o$.

[d] Mesopore volume determined using the BJH method in the range 3.5–170 nm.

3.3. Hydrogen Chemisorption

The results of hydrogen chemisorption measurements conducted on the metal-loaded samples are presented in Table 2. For ease of comparison, selected chemisorption results from the fresh samples presented in part 1 of this work are included. Notwithstanding the initial apparent differences in H_2 uptake at 308 K due to the presence of chloride, similar qualitative behaviour is exhibited by both samples. MT reduction—without an intermediate oxidation—dramatically decreases the H_2 uptake at both 308 and 195 K to similar values.

Oxidation at 700 K followed by reduction at 373 K partially restores the H_2 uptake for both samples and at both temperatures of investigation. The extent of recovery is higher in the case of Rh/CeZr (Cl), reaching ca. 66% of

TABLE 2

Volumetric Hydrogen Adsorption on $Rh/Ce_{0.6}Zr_{0.4}O_2$ Samples

Catalyst	Oxidation temperature (K)[a]	Reduction temperature (K)	H_2 uptake ($\mu mol\ g^{-1}$)		H/Rh	
			308 K	195 K	308 K	195 K
$Rh/Ce_{0.6}Zr_{0.4}O_2$ (N)	—	423[b]	133.4	9.8	5.48	0.40
	—	1073[c]	4.0	4.0	0.15	0.17
	700	373[c]	66.0	4.9	2.72	0.23
	700	523[c]	9.4	4.9	0.38	0.23
	—	1273[b,d]	0.4		0.03	
	700	423[c]	11.2		0.46	
	923	423[c]	18.7	3.8	0.77	0.16
	1023	423[c]	16.1		0.65	
	1173	423[c]	10.3		0.43	
$Rh/Ce_{0.6}Zr_{0.4}O_2$ (Cl)	—	423[b]	24.5	9.4	1.01	0.38
	—	1073[c]	3.6	3.6	0.14	0.16
	700	373[c]	16.1	5.4	0.66	0.23
	700	523[c]	5.4	5.4	0.24	0.23
	—	1273[b,d]	0.4		0.03	

[a] Sample reoxidised (5% O_2/He 1 h) at indicated temperature before reduction and chemisorption measurement.

[b] Sample pretreated in O_2 (5%)/ He at 900 K for 0.5 h before reduction.

[c] Sample from previous run.

[d] Sample used in TPR–MS experiments prior to chemisorption measurements.

its original values at both temperatures of investigation (H/Rh = 0.66 and 0.23), as compared to ca. 50% for the Rh/CeZr (N) measurements (H/Rh = 2.72 and 0.23). However, it should also be noted that the recovery observed in terms of the amount of hydrogen uptake is considerably larger in the case of Rh/CeZr (N).

A further oxidation at 700 K followed by reduction at 523 K results in a decrease in H_2 chemisorption, but only at 308 K. The values obtained at 195 K are the same as those obtained after pre-reduction at 373 K. For Rh/CeZr (Cl) the chemisorption value obtained at 308 K after reduction at 523 K reverts back to the same value as that obtained at 195 K (H/Rh = 0.24), while for Rh/CeZr (N) a higher uptake is observed (H/Rh = 0.38).

HT reduction suppresses H_2 chemisorption almost completely. The effects of reoxidation and subsequent LT reduction were investigated for Rh/CeZr (N) in some detail. Two main points emerge from this investigation. First, reoxidation at 923 K followed by reduction at 423 K leads to a H/Rh value measured at 195 K of 0.16, which is slightly lower than those measured at the same temperature after oxidation at 700 K and reduction at 373 or 523 K in earlier runs (H/Rh = 0.23). Second, for measurements conducted at 308 K, there seems to be an optimal oxidation temperature around 900 K leading to the higher H/Rh = 0.77 value among this set of experiments.

3.4. Temperature-Programmed Reduction

TPR–MS profiles of the fresh and HT cycled samples are presented in Fig. 3. Note that up to four redox cycles were carried out on all the samples. Since no further changes were detected after the first recycle, only the first two profiles obtained from each material are reported. The support exhibits single H_2 uptake and H_2O desorption peaks for both the fresh and recycled samples. However, the positions of hydrogen minima and water maxima, which closely coincide in the individual experiments, shift from 875 K in the profile of the fresh sample (Fig. 3, traces 1a and 1b) to 930 K in that of the recycled sample (Fig. 3, traces 2a and 2b).

The presence of the metal substantially decreases the positions of maximum H_2 uptake and H_2O evolution. For the fresh samples, both H_2 uptake and H_2O production start somewhat earlier for Rh/CeZr (N) than for Rh/CeZr (Cl). However, after HT cycling a similar overall behaviour is evident for the samples. For Rh/CeZr (N) the maximum of hydrogen uptake increases from 370 to 480 K (Fig. 3, traces 5a and 6a), while the maximum of water evolution increases from 420 to 550 K (Fig. 3, traces 5b and 6b). Water evolution commences somewhat earlier in the recycled sample. Similar observations may be made in the case of Rh/CeZr (Cl): the maximum of hydrogen uptake shifts from 420 to 480 K (Fig. 3, traces 3a and 4a), while the maximum of water evolution increases from 360 to 570 K (Fig. 3, traces 3b and 4b). With regard to the latter, it should be noted that there is a point of inflection in water evolution near 470 K (Fig. 3, trace 4b), and water production is high and increasing slowly thereafter up to 570 K. After recycling it is also possible to distinguish a contribution from rhodium oxide reduction near 350 K (Fig. 3, traces 4a and 4b). The asymmetric appearance of the peaks due to water evolution is somewhat unusual. We tentatively attributed these phenomena to some kind of chromatographic effect due to the necessity of using relatively high amounts of catalysts. Consistently, the fresh sample, i.e., unsintered, shows a continuous evolution of water, indicating retention of water at the support surface.

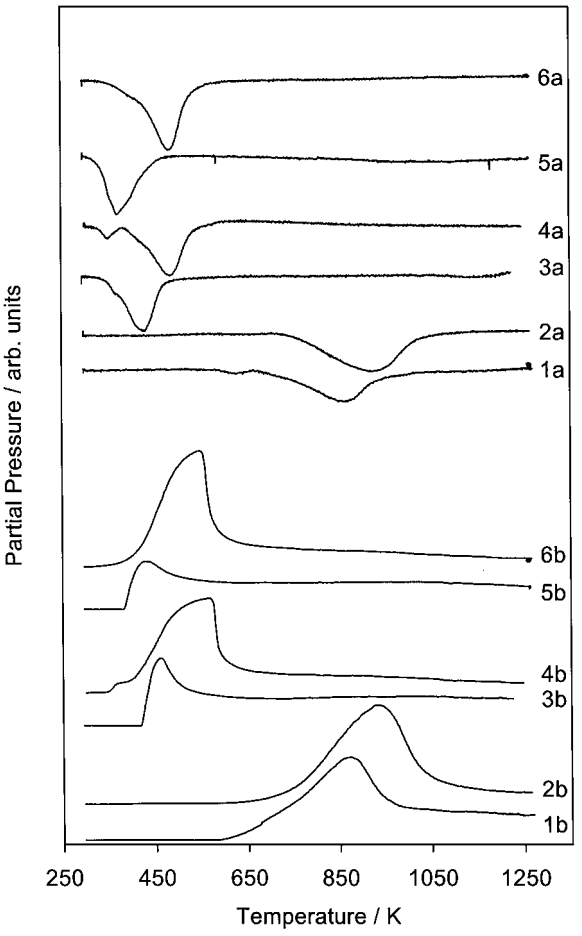

FIG. 3. Hydrogen uptake (a) and water evolution (b) obtained during TPR–MS profiles of (1) $Ce_{0.6}Zr_{0.4}O_2$, fresh; (2) $Ce_{0.6}Zr_{0.4}O_2$, HT-cycled; (3) $Rh/Ce_{0.6}Zr_{0.4}O_2$ (Cl), fresh; (4) $Rh/Ce_{0.6}Zr_{0.4}O_2$ (Cl), HT-cycled; (5) $Rh/Ce_{0.6}Zr_{0.4}O_2$ (N), fresh; (6) $Rh/Ce_{0.6}Zr_{0.4}O_2$ (N), HT-cycled.

The results of oxygen uptake experiments at 700 K after HT reduction are summarised in Table 3. The uptake shown the recycled samples is an average of three such reoxidation procedures. Remarkable stability of the OSC values measured was observed in these experiments. CeZr exhibits an average uptake of 816 μmol of O_2 g^{-1}. For the Rh-loaded

TABLE 3

O_2 Uptake Measured at 700 K after TPR Experiments

Sample	No. of cycle	Treatment	O_2 uptake[a] (μmol g^{-1})	Ce^{3+} (%)
$Ce_{0.6}Zr_{0.4}O_2$	1	HT	816	77
	2→4		816	
$Rh/Ce_{0.6}Zr_{0.4}O_2$ (N)	1	HT	937	84[b]
	2→4		937	
$Rh/Ce_{0.6}Zr_{0.4}O_2$ (Cl)	1	HT	915	82[b]
	2→4		915	

[a] Standard deviation, ± 9 μmol g^{-1}.

[b] Value corrected for the presence of metal, assuming full reoxidation of all nominal rhodium loading from Rh^0 to Rh_2O_3.

samples the O_2 uptake values increase to 937 μmol of O_2 g^{-1} for Rh/CeZr (N) and 915 μmol of O_2 g^{-1} for Rh/CeZr (Cl). Correction for the presence of the metal reduced these values to 897 and 874 μmol of O_2 g^{-1}, respectively. Such a difference is rather small. These values correspond to higher degrees of ceria reduction (84 and 82%) than in the case of the pure support (77%), which in turn corresponds to an increase of the total oxygen storage capacity (OSC) of the samples.

3.5. Temperature-Programmed Desorption of H_2

A comparison of the effect of HT reduction on TPD–MS of hydrogen adsorbed at 308 K from Rh/CeZr (N) and Rh/CeZr (Cl) is reported in Fig. 4. The TPDs from the fresh samples presented in part 1 are also included. The latter profiles were recorded after the following procedure: reduction at 423 K, hydrogen exposure at 308 K and, finally, TPD to 873 K. For the HT reduced samples, the procedure involved reduction at 1273 K followed by flushing in He at this temperature before cooling to the adsorption temperature (without an intermediate oxidation step).

With respect to reversibly adsorbed hydrogen (Fig. 4), the most striking feature is that the HT reduction almost completely eliminates the previously observed high-temperature peaks at 550 K for Rh/CeZr (N) and 630 K for Rh/CeZr (Cl). The presence of the low-temperature feature at ca. 350 K indicates that there is exposed metal surface still available after reduction at 1273 K. Similar behaviour was observed after reduction at 1073 K (as outlined below). Subsequent reoxidation at 700 K and re-reduction at 423 K almost completely suppresses the reversible hydrogen adsorption of Rh/CeZr (N) (Fig. 4) and of Rh/CeZr (Cl) (see below). In contrast with the fresh samples the HT cycled samples exhibit no H_2O desorption.

The effect of oxidation on the TPD behaviour after MT or HT reduction was further investigated in the case of Rh/CeZr (Cl). These experiments are summarised in Fig. 5. Adsorption of H_2 at 308 K after reduction 1073 K (as in the chemisorption measurements) produces a profile similar to those observed in Fig. 4 after HT treatment, viz., a single peak at 360 K. Subsequent oxidation at 700 K followed by a reduction at 423 K results in an almost complete suppression of hydrogen desorption. Further cycles consisting of high-temperature reduction, reoxidation at 700 K, and reduction at increasing temperatures (373, 473, and 573 K) progressively restore the H_2 desorption profiles obtained, which begin to resemble those obtained for the low-temperature cycled samples (Fig. 4). However, it is significant that there is no water desorption in any of these experiments.

Semiquantitative analysis of the H_2 desorption reveals that the total desorption amounts are 17 (trace 1a), 14 (trace 1b), 47 (trace 2a), 17 (trace 2b), and 3 (trace 2c) μmol g^{-1} in Fig. 4, and 35 (trace 1), 2 (trace 2), 21 (trace 3), 3 (trace 4), 13 (trace 5), and 21 (trace 6) μmol g^{-1} in Fig. 5.

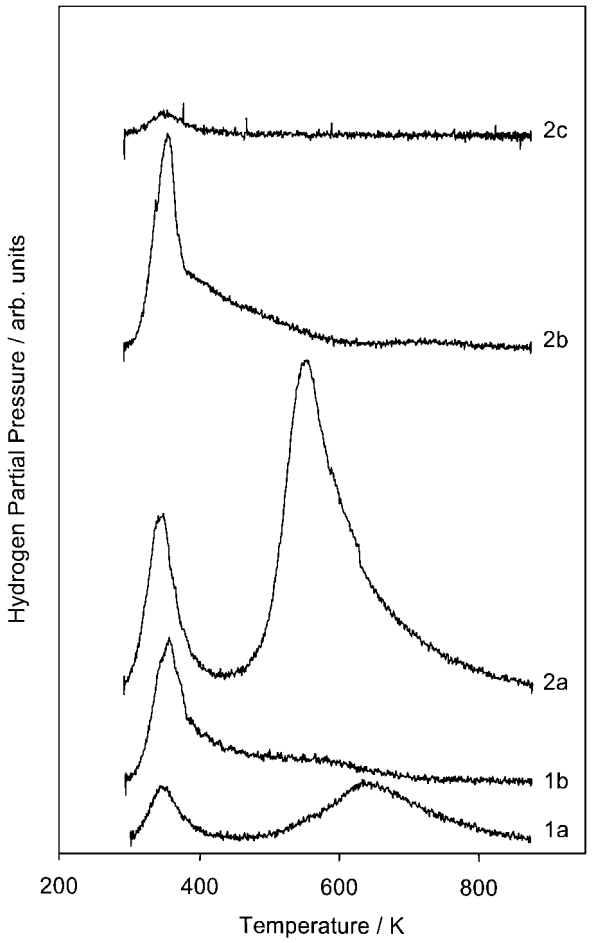

FIG. 4. Comparison of H_2 desorption profiles from $Rh/Ce_{0.6}Zr_{0.4}O_2$ (N) and $Rh/Ce_{0.6}Zr_{0.4}O_2$ (Cl) following exposure to a flow of 5% H_2 in Ar at 308 K after various treatments: (1) $Rh/Ce_{0.6}Zr_{0.4}O_2$ (Cl), (a) fresh and (b) after HT reduction; (2) $Rh/Ce_{0.6}Zr_{0.4}O_2$ (N), (a) fresh and (b) after HT reduction; (2c) sample from (2b) followed by oxidation at 700 K and reduction at 423 K.

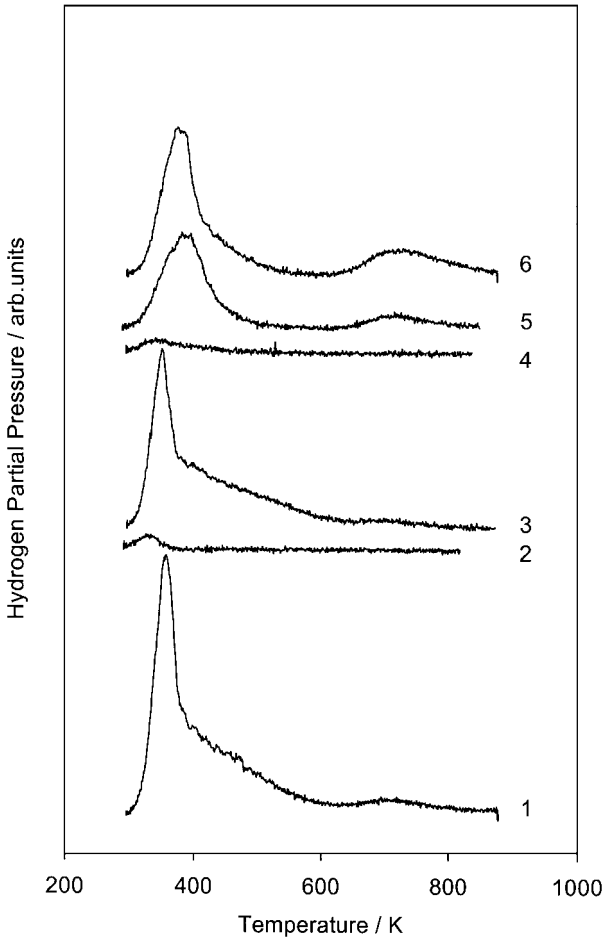

FIG. 5. Comparison of H_2 desorption profiles from $Rh/Ce_{0.6}Zr_{0.4}O_2$ (Cl) following exposure to a flow of 5% H_2 in Ar at 308 K after a sequence of various treatments: (1) MT reduction; (2) reoxidation at 700 K and reduction at 423 K; (3) HT reduction; (4) reoxidation at 700 K and reduction at 373 K; (5) reoxidation at 700 K and reduction at 473 K; (6) reoxidation at 700 K and reduction at 573 K.

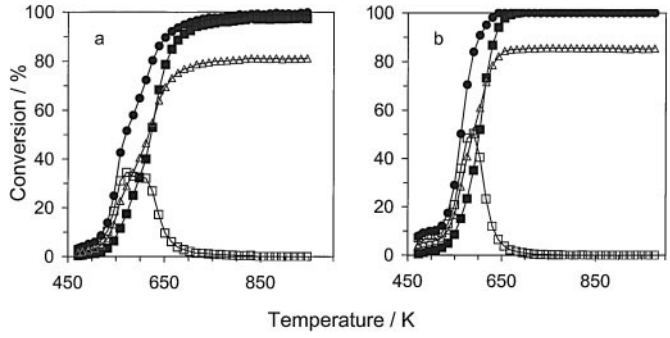

FIG. 6. Temperature-programmed reaction profile of the CO + NO reaction over (a) fresh $Rh/Ce_{0.6}Zr_{0.4}O_2$ (Cl) and (b) fresh $Rh/Ce_{0.6}Zr_{0.4}O_2$ (N): (●) NO conversion, (■) conversion of NO to N_2, (□) conversion of NO to N_2O, and (△) CO conversion. For clarity, only data recorded up to 973 K are plotted. No further changes in conversion levels were observed above the range shown.

3.6. Catalytic Activity Measurements

The results of catalytic activity tests performed on the two metal-loaded samples are summarised in Table 4. Figure 6 depicts the activity profiles obtained during the first ramping procedure described in the Experimental section. With regard to the light-off temperatures of CO and NO, no clear trend emerges during progressive ageing of the samples, and these light-off values may be regarded as being constant. With the exception of the peak intensity for Rh/CeZr (Cl) during the first temperature-programmed reaction, this is also true of the intensity and position of N_2O formation. The lower value of the maximum of N_2O formation during the first cycle is due to a plateau in its production (Fig. 6a) which does not exist in the case of Rh/CeZr (N) (Fig. 6b). This plateau is absent in subsequent cycles. However, the results of isothermal measurements conducted at 473 K under a kinetically controlled regime reveal a strong distinction between the samples. Throughout the sequence the rate values obtained for Rh/CeZr are approximately

TABLE 4

NO + CO Activity on $Rh/Ce_{0.6}Zr_{0.4}O_2$ (N) and $Rh/Ce_{0.6}Zr_{0.4}O_2$ (Cl)

Catalyst	Run[a]	Rate of formation at 473 K[b] ($(mol\ g_{cat}^{-1}\ s^{-1}) \times 10^8$)			Light-off temperature[c] (K)		N_2O formation	
		N_2	N_2O	CO_2	N_2	CO_2	Peak maximum (%)	Temperature (K)
$Rh/Ce_{0.6}Zr_{0.4}O_2$ (N)	1	25	126	174	602	588	51	590
	2	13	36	60	608	587	55	582
	3	10	28	44	607	590	59	585
$Rh/Ce_{0.6}Zr_{0.4}O_2$ (Cl)	1	13	50	76	622	617	34	572
	2	6	19	28	605	591	64	585
	3	5	15	22	608	593	64	585

[a] Consecutive experiments. The reported data were measured after 10 h of reaction.
[b] Rate measurements were made under differential conditions. A lean reaction mixture was used. CO : NO = 1.2 : 1.
[c] Defined as the temperature at which 50% of conversion of reactants is observed.

50% lower than the corresponding Rh/CeZr(N) values. The effect of ageing on the overall behaviour is that the activities of the samples decrease. However, rate differences persist even on the third reaction cycle.

4. DISCUSSION

High-temperature reduction is known to significantly alter the textural properties of ceria and ceria–zirconia materials (5, 6). These effects include mainly sintering of both the metal and support particles, dehydroxylation of the support, and decoration or coverage of the metal particles by reduced support. With regard to the last point, Bernal and co-workers (7, 8) have demonstrated in a series of papers that Rh/CeO_2 does not enter into a classical SMSI state, as originally defined by Tauster *et al.* (9, 10) for Rh/TiO_2, unless reduction temperatures greater than 973 K are adopted. Instead they attribute SMSI-like effects observed at lower temperatures to dehydroxylation of the support at temperatures above 623 K (11). With a few exceptions, most of the work done in this regard has focussed on NM/CeO_2 systems, and the behaviour of ceria–zirconia supported samples in these regards is therefore less well-established (12, 13). In addition, ceria–zirconia systems show unique effects after high-temperature reducing or oxidising treatments, mainly in strong modifications on the redox behaviour (5, 14). The present investigation focuses on the effect of severe reduction treatments on such behaviour. While the effect of high-temperature cycling has recently been considered (12, 13, 15), the effect of precursor has not as yet been addressed.

As was the case in part 1 of this work, an important point to remember throughout the following discussion is that chemical analysis indicates that chloride is retained even after HT reduction. In addition, the previous results indicate that the fresh Rh-loaded materials differ only in the presence of chloride.

4.1. Textural Analysis

It is clear from the data presented that the high-temperature treatments applied to the samples result in a progressive sintering of the samples. Although these results pertain largely to the support, sintering of the metal must also occur to accommodate the observed changes. However, there is no significant dependence on the nature of the precursor used. In fact, the behaviour of the support closely mirrors that of the Rh-loaded samples, indicating that the changes which occur are independent of the presence of the metal. This apparently contradicts a previous observation that Rh stabilises both CeO_2 and $Ce_{0.5}Zr_{0.5}O_2$ against surface area collapse under thermal/reductive conditions (12). However, different reduction temperatures (1000 vs 1273/1073 K) and a different mixed oxide precursor were used in that study, which could easily account for the apparently different behaviour.

4.2. Temperature-Programmed Reduction

With regard to the TPR–MS profiles (Fig. 3), while the presence of Rh produces the well-established overall decrease in the reduction temperature, it is of interest to note that the qualitative behaviour of support reduction is the same for all the samples. High-temperature reductive ageing during the initial TPR results in a shift to higher temperatures of the positions of maximum H_2O formation H_2 uptake, although H_2O formation does appear earlier. Previous investigations have reported that upon redox cycling such as that employed here, different reduction behaviour may be obtained, including lowering of reduction temperatures (5, 14). The exact origin of these phenomena has still to be ascertained, since multiple parameters such as structural/textural properties and even pretreatments may play an important role.

The behaviour here observed is in contrast to that observed after LT cycling (1), after which the positions of both H_2 uptake and initial H_2O formation were lowered. HT cycling largely eliminates distinction of Rh/CeZr (N) and Rh/CeZr (Cl) by the TPR technique. A distinction was possible during LT experiments, mainly in terms of H_2 uptake. The question of H_2 interaction with the support will be discussed in more detail below. As before, a lag always exists between H_2 uptake and H_2O production, indicating that these variables are not directly linked.

The results of classical TPR experiments obtained prior to reoxidation at 700 K confirm the hydrogen uptake observations outlined above. The O_2 uptake measurements demonstrate that the degree of reduction reached upon HT reduction does not show a dependence on the precursor used, but the metal-loaded samples undergo a higher degree of reduction than the support. This illustrates the absence of any appreciable chloride effect on the degree of vacancy creation in the samples upon severe reduction.

4.3. Chemisorption

Chemisorption experiments reveal a dramatic dependence of H_2 interaction with both Rh/CeZr (N) and Rh/CeZr (Cl) on the MT and HT reductive pretreatments. After MT reduction, the similarity in the values of H/Rh (0.14–0.17) obtained for both samples at both temperatures of investigation is a strong indication that spillover is completely blocked and that the H/Rh values obtained very likely closely reflect the true adsorption of H_2 on exposed Rh. Thus, site blocking by the retained chloride should not be a factor. Dehydroxylation of the support, resulting in an inhibition of spillover, is the most likely explanation for this effect, although, as will be outlined below, interesting differences exist between the chemisorption and TPD–MS results that show that the situation is not entirely straightforward. The H_2 uptake values measured are not negligible and demonstrate that the system has not entered into a classical

SMSI state after reduction at this temperature. However, metal decoration effects cannot be ruled out. As suggested by a referee, embedding of the particles in the support micropores could furnish an explanation for the decreases. The further decreases of the H_2 chemisorption values measured (at 308 K) upon HT reduction are attributable to a high degree of decoration of the metal. In view of the above-discussed effects of MT reduction, complete suppression of spillover is likely. The possibility of such effects upon HT and MT reduction of the samples is supported by the textural analysis data, which show progressive modification of the support upon increasing the temperature of reduction.

After the MT reduction, the partial recovery of H_2 uptake upon reoxidation at 700 K and reduction at 373 K (mild procedures) may be explained by rehydroxylation of the support and/or redispersion of the metal due to the oxidative treatment. However, the extent of recovery differs for Rh/CeZr (N) and Rh/CeZr (Cl). In addition, oxidation at 700 K followed by reduction at 523 K results in a decrease in H_2 uptake for both samples 308 K, but to different extents. Such decreases in the H_2 uptake may be attributed to a decrease in the rate of H_2 spillover due to dehydroxylation of the surface induced by the higher reduction temperature. The differences between Rh/CeZr (N) and Rh/CeZr (Cl) may be attributed to the effect of retained chloride. In the case of Rh/CeZr (Cl), reduction at 523 K results in a decrease of the uptake value to that attributed to metal-adsorbed H_2, but this is not the case for Rh/CeZr (N). Therefore, in contrast to Rh/CeZr (N), it would appear that, for the MT cycled Rh/CeZr (Cl) sample, spillover can be eliminated by reduction at 523 K. For Rh/CeZr (N), the dependence of the values measured for H/Rh after reduction at 423 K on reoxidation temperature is an interesting observation and, in accord with previous observations and the above discussion, further illustrates the impact of pretreatment on redox phenomena (5, 12, 16).

4.4. Temperature-Programmed Desorption

After HT reducion, the absence of peaks previously attributed to back-spillover from the support (1) suggests a degree of dehydroxylation of the samples, besides their strong sintering. However, interesting differences emerge in a comparison of the behaviour of the chemisorption and TPD experiments. Semiquantitative analysis of the TPD peak indicates that, after HT reduction, the amount of H_2 desorbed during TPD is significantly higher than the amount chemisorbed at the same temperature. It should be noted that, in comparison to the total amount of H_2 adsorbed after LTR (reversible and irreversible), the reversible-only adsorption in the present case is small, however. Nevertheless, this difference is an unexpected finding and merits some comment. In view of the attribution of the H_2 uptake in the chemisorption experiments to metal-only adsorbed hydrogen, and the previous attribution of the first TPD peak to metal and near-metal adsorbed H_2 (1), an implication is that in the TPD methodology somehow allows hydrogen to adsorb on the near metal sites. A reasonable explanation for this phenomenon might be found in the strengths of the H_2 removal procedures employed (vacuum vs flow at reduction temperature). This could be a crucial point, since it has been observed that vacuum treatment may lead to reoxidation of Rh/CeO_2 by desorption of H_2 (17, 18). In addition to the possibility that the observations are due to different degrees of dehydroxylation induced by the nonequivalent pretreatment procedures, it should also be considered that they could be related to the very different conditions of adsorption, which might be expected to affect the kinetics of spillover. The behaviour highlights the extreme sensitivity of these materials to pretreatment/methodology and signals that caution should be exercised when extrapolating data obtained in chemisorption experiments to TWC applications, as the conditions are considerably different.

This sensitivity is further illustrated by apparent conflicts between chemisorption and TPD–MS results in the sequences of experiments conducted using Rh/CeZr (Cl) which involved oxidation followed by reduction at various temperatures (Fig. 5, Table 1). In the case of the TPD–MS results, following MT and HT treatments, reoxidation followed by low-temperature reduction almost completely eliminates H_2 desorption. Increasing the reduction temperature during the following redox cycles progressively increases the amount of H_2 desorption, with the gradual reappearance of the higher temperature H_2 desorption peak. This may be attributed to rehydroxylation of the surface. On the other hand, in the chemisorption experiments the H_2 uptake first increases and then decreases upon increasing the reduction temperature. As this is again attributable to different degrees of hydroxylation of the surface induced by the reductive treatments, these results indicate a very complicated dependence of hydrogen uptake measurements on the exact methodology employed. Note, however, that hydrogen storage in the sample, which is not desorbed under flow (at room temperature), could also furnish a reasonable explanation for all of these observations.

The absence of H_2O desorption from any profiles obtained after reduction at elevated temperatures is in contrast with the LT cycled samples which showed significant H_2O desorption during TPD–MS experiments. As the main difference between the samples is the surface area, this might be taken to indicate that reduction during the TPD is a surface phenomenon.

4.5. Activity Measurements

Important evidence of the effect of retained chloride even after prolonged ageing under reaction conditions is

provided by the rate measurements. Rh/CeZr (Cl) does show some evidence of chloride removal from the first to the second temperature-programmed reaction, as the shape of the N_2O formation peak changes. However, the fact that a constant difference of ca. 50% between the rates of formation of products for the two samples is maintained throughout the series of experiments demonstrates that chloride retention has significant influence on the activity of these materials and that sufficient chloride removal to affect activity behaviour is not facile. Decrease of activity due to residual chloride retained on the support is in agreement with the idea that the support is significantly involved, through its redox properties, in the mechanism of the reaction (19). Consistent with this previous work, above 500 K no appreciable differences are found between the two catalysts, since Rh-only catalysed reaction was suggested to occur under those conditions.

5. CONCLUSIONS

The results demonstrate that the identity of the rhodium precursor used has no significant bearing on the degree of vacancy creation in the samples upon application of identical high-temperature reduction procedures. In terms of sample reduction, the severity of the reduction procedure has a more significant effect on the behaviour observed, affecting the position of vacancy creation. However, effects of retained chloride on activation of hydrogen species are detectable even after the high-temperature cycling procedure. This is evident in the chemisorption behaviour at low temperature. More importantly, the catalytic behaviour observed in the reduction of NO by CO indicates that, despite prolonged ageing under reaction conditions, retained chloride has a detrimental effect on the conversions observed. Therefore, under realistic TWC operating conditions, catalytic behaviour may be affected by the presence of retained chloride, most probably by modification of the redox properties of the support. This re-emphasises the unsuitability of chloride-based preparations for TWC applications and indicates that very severe cleaning/ageing procedures may be necessary to fully remove adsorbed chloride.

ACKNOWLEDGMENTS

Prof. C. Dossi, Università dell'Insubria (Como, Italy) is gratefully acknowledged for chemical analyses. University of Trieste, the Ministero dell'Ambiente (Roma), Contract DG 164/SCOC/97, CNR (Roma) Programmi Finalizzati "Materiali Speciali per Tecnologie Avanzate II", Contract 97.00896.34, and MURST (Roma) "Progetti di Ricerca di Rilevante Interesse Nazionale—1998" are gratefully acknowledged for financial support.

REFERENCES

1. Fornasiero, P., Hickey, N., Kašpar, J., Dossi, C., Gava, D., and Graziani, M., *J. Catal.* **189**, 326 (2000).
2. Kappers, M., Dossi, C., Psaro, R., Recchia, S., and Fusi, A., *Catal. Lett.* **39**, 183 (1996).
3. Sing, K. S. W., Everett, D. H., Haul, R. A. W., Moscou, L., Pierotti, R. A., Rouquerol, J., and Sieminiewska, T., *Pure Appl. Chem.* **57**, 603 (1985).
4. Barret, E. P., Joyner, L. G., and Halenda, P. P., *J. Am. Chem. Soc.* **73**, 373 (1951).
5. Fornasiero, P., Balducci, G., Di Monte, R., Kašpar, J., Sergo, V., Gubitosa, G., Ferrero, A., and Graziani, M., *J. Catal.* **164**, 173 (1996).
6. Perrichon, V., Laachir, A., Abouarnadasse, S., Touret, O., and Blanchard, G., *Appl. Catal. A Gen.* **129**, 69 (1995).
7. Bernal, S., Botana, F. J., Calvino, J. J., Cifredo, G. A., and Perez-Omil, J. A., *Catal. Today* **23**, 219 (1995).
8. Bernal, S., Calvino, J. J., Cauqui, M. A., Perez-Omil, J. A., Pintado, J. M., and Rodriguez-Izquierdo, J. M., *Appl. Catal. B Environ.* **16**, 127 (1998).
9. Tauster, S. J., Fung, S. C., and Garten, R. L., *J. Am. Chem. Soc.* **100**, 170 (1978).
10. Tauster, S. J., and Fung, S. C., *J. Catal.* **55**, 29 (1978).
11. Bernal, S., Calvino, J. J., Cifredo, G. A., Laachir, A., Perrichon, V., and Herrmann, J. M., *Langmuir* **10**, 717 (1994).
12. Fornasiero, P., Kašpar, J., Sergo, V., and Graziani, M., *J. Catal.* **182**, 56 (1999).
13. Kašpar, J., Fornasiero, P., and Graziani, M., *Catal. Today* **50**, 285 (1999).
14. Balducci, G., Fornasiero, P., Di Monte, R., Kašpar, J., Meriani, S., and Graziani, M., *Catal. Lett.* **33**, 193 (1995).
15. Fornasiero, P., Kašpar, J., and Graziani, M., *J. Catal.* **167**, 576 (1997).
16. Baker, R. T., Bernal, S., Blanco, G., Cordon, A. M., Pintado, J. M., Rodriguez-Izquierdo, J. M., Fally, F., and Perrichon, V., *Chem. Commun.* 149 (1999).
17. Bernal, S., Calvino, J. J., Cifredo, G. A., Rodriguez-Izquierdo, J. M., Perrichon, V., and Laachir, A., *J. Catal.* **137**, 1 (1992).
18. Bernal, S., Calvino, J. J., Cifredo, G. A., Rodriguez-Izquierdo, J. M., Perrichon, V., and Laachir, A., *J. Chem. Soc., Chem. Commun.* 460 (1992).
19. Fornasiero, P., Ranga Rao, G., Kašpar, J., L'Erario, F., and Graziani, M., *J. Catal.* **175**, 269 (1998).